



## Electrochemical Deposition of ZnO Thin Films on to Tin(IV) oxide:Fluorine

M. YILMAZ<sup>1,2,\*</sup>, G. TURGUT<sup>3</sup>, S. AYDIN<sup>1</sup> and M. ERTUGRUL<sup>1</sup>

<sup>1</sup>Department of Nanoscience and NanoEngineering, Graduate School of Natural and Applied Sciences, Ataturk University, Erzurum 25240, Turkey

<sup>2</sup>Department of Physics, Faculty of Science and Arts, Bingol University, Bingol 12000, Turkey

<sup>3</sup>Department of Physics, Graduate School of Natural and Applied Science, Ataturk University, Erzurum 25240, Turkey

\*Corresponding author: Fax +90 44 22369055; Tel: +90 44 22314011; E-mail: mehmetyilmaz@atauni.edu.tr

(Received: 23 June 2011;

Accepted: 6 March 2012)

AJC-11145

In this study firstly, fluorine doped tin(IV) oxide thin film was formed on glass substrate by spray pyrolysis method. Then ZnO film was growth by electrochemical deposition onto conductive fluorine doped tin(IV) oxide film sprayed and ZnO thin films were annealed in air at 450 °C. The crystal structures of fluorine doped tin(IV) oxide and ZnO thin films was characterized with XRD. It was identified that fluorine doped tin(IV) oxide and ZnO films had cassiterite and hexagonal wurtzite structure, respectively. Surface morphology of annealed and unannealed ZnO was characterized by SEM. According to SEM analysis, annealed ZnO thin film compared to the unannealed film has a homogeneous surface morphology and small grains. Also, electrical measurement of the obtained FTO/ZnO/Au structure investigated by I-V measurements. Series resistance, barrier height and ideality factor values of obtained structure were calculated and discussed from I-V measurements.

**Key Words:** *n*-ZnO, Electrochemical deposition, Spray pyrolysis.

### INTRODUCTION

Zinc oxide is generally called a II-VI semiconductor because zinc and oxygen belong to the 2nd and 6th groups of the periodic table. Zinc oxide has a important properties that is good transparency, high electron mobility *etc.* Zinc oxide is a *n*-type semiconductor and has a 3.2 eV band gap<sup>1</sup>. From these properties ZnO semiconductor use of wide range application such as magnetoelectronics, nanotechnology, optoelectronics<sup>2-5</sup>. Nowadays, ZnO nanostructures are very attractive because of nanotechnological applications be important. Zinc oxide nanostructures are generally prepared using the sol-gel, polymer stablization, electrodeposition, spray pyrolysis technique *etc.*<sup>6,7</sup>.

Electrodeposition of the semiconducting materials thus represent a new challenge, not only from the academic point of view but also from the economic point of view, since this method presents interesting characteristic for large area, low cost and generally low temperature and soft processing of materials<sup>8</sup>. The structural and optical properties of ZnO thin films depend on the preparation methods, substrate temperature, substrate materials and subsequent annealing treatment. The most important of these the choice of the substrate because matching in lattice parameters and crystal structure between

the film and substrate strongly affect the crystal growth behaviour<sup>9</sup>. Fluorine doped tin(IV) oxide (FTO), which is used as one of the substrates in preparation of ZnO nanostructures with electrodeposition, has many important properties such as low electrical resistivity, high optical transmittance in visible region, high optical reflectance in infrared region, chemically inert and mechanically hard<sup>10</sup> further, fluorine doped tin(IV) oxide thin films are stable up to high temperatures, have excellent resistance to strong acids and they have very good adhesion to many substares<sup>11-13</sup>. Various technique have been developed for TCO's thin film depositions. Sol-gel, chemical vapour deposition, spray pyrolysis, pulsed laser deposition are currently used for preparation of fluorine doped tin(IV) oxide thin films<sup>14</sup>. Spray pyrolysis technique is simple than the other technique because of this spray pyrolysis technique is very attractive technique than the other technique.

In this study, fluorine doped tin(IV) oxide was grown on glass substrate by spray pyrolysis technique. Then ZnO was grown on to fluorine doped tin(IV) oxide by electrochemical deposition technique crystal structures of fluorine doped tin(IV) oxide and ZnO are characterized by XRD and surface morphology characterized by SEM. As a result we have obtained structures like nano-wire and electrical properties of the ZnO thin film were investigated.

## EXPERIMENTAL

Firstly 0.9 M  $\text{SnCl}_2 \cdot 2\text{H}_2\text{O}$  was dissolved in hydrochloric acid (HCl) by heating for 10 min. This mixture subsequently diluted with methanol served as starting solution. The addition of HCl was required in order to break down the polymer molecules that were formed when diluting with methanol<sup>15</sup>. For fluorine doping, ammonium fluoride dissolved in doubly distilled water was added with the starting solution. The weight percentage of (F)/(Sn) ratio in the spray solution were 20. The spray solution was magnetically stirred for 1 h and finally this solution was filtered by syringe filter with 0.2  $\mu\text{m}$  pore size before spraying on substrate. The well-cleaned microscopic glasses with 1 cm  $\times$  1 cm  $\times$  1mm dimensions were used as substrates. Electrochemical stage of the study the electrochemical cell used for this study consisted of a three-electrode system and a Gamry Reference 3000 workstation. The working electrodes were fluorine doped tin(IV) oxide coated glass substrates. The counter electrode was a platinum wire and Ag/AgCl was served as reference electrode. The electrolytic solutions were prepared from following composition: 0.1 M  $\text{Zn}(\text{NO}_3)_2 \cdot 6\text{H}_2\text{O}$  and 0.1 M KCl. The solution was heated on a hotplate and voltage of 1.1 V was applied for 2 min when the temperature of the solution reached 65 °C. The temperature of the solution and the applied voltage were maintained constant through the deposition time.

Crystal structure was evaluated by Rigaku D/Max-IIIIC diffractometer from  $2\theta = 10^\circ$  to  $90^\circ$  with  $\text{CuK}\alpha$  radiation ( $\lambda = 1.5418 \text{ \AA}$ ), at 30 kV, 10 mA. The morphological properties and electrical properties were investigated by SEM and I-V techniques, respectively. To obtain electrical measurements, it was made Au contacts on annealed FTO/ZnO structure by sputtering technique Fig. 1(a) and (b) shows the band diagram of glass/FTO/ZnO/Au device where  $W$  is depletion region and  $\phi_b$  is work function of the metal. While  $\phi_b$  is being constant at metal region it changes depending on fed at semiconductor region.

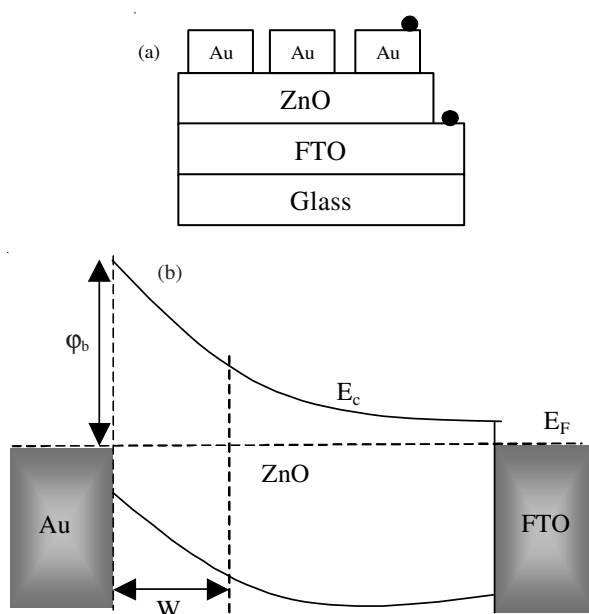


Fig.1. Schematic diagram for glass/FTO/ZnO/Au device and band diagram<sup>16</sup>

## RESULTS AND DISCUSSION

**XRD analysis:** The crystal structures of obtained samples were investigated by XRD (Fig. 2). XRD images showed that fluorine doped  $\text{SnO}_2$  thin film was polycrystalline with cassiterite structure (PDF card No:41-1445). Zinc oxide thin films were polycrystalline with hexagonal wurtzite structure (PDF card no: 36-1451). For hexagonal structure, the lattice constant 'a' and 'c' was determined by eqn. (1)<sup>1</sup>.

$$d = \frac{1}{\sqrt{\frac{4}{3a^2}(h^2 + hk + k^2) \frac{l^2}{c^2}}} \quad (1)$$

where 'd' is the interplaner distance and (hkl) miller indices, respectively.

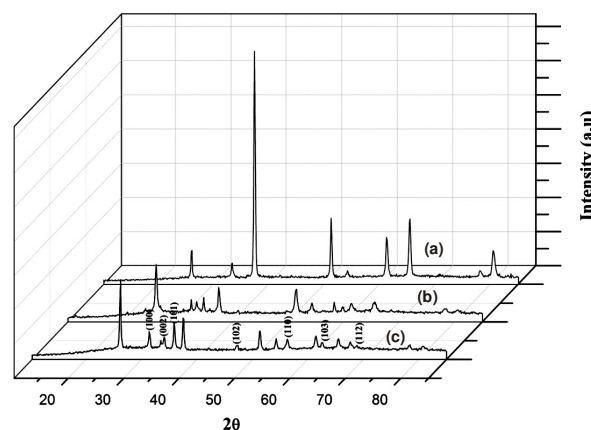


Fig. 2. XRD pattern of samples a) Pure FTO; b) FTO/ZnO; c) FTO/ZnO annealed in air at 450 °C

The standard and calculated lattice constants were given in Table-1. The calculated 'a' and 'c' values agree with standard values obtained from PDF Card No:36-1451.

TABLE-1  
STRUCTURAL PARAMETERS OF UNANNEALED  
AND ANNEALED ZnO

Sample	Calcd. lattice constants (Å)		
	a	c	c/a
Unannealed ZnO	3.18	5.20	1.63
Annealed ZnO for 3h at 450 °C in air	3.29	5.26	1.59

\*PDF card no: 36-1451 (a\* = 3.250 Å c\* = 5.207 Å)

**SEM analysis:** The average particle size was calculated using by Scherrer formula (eqn. 2.)<sup>17</sup>;

$$D = \frac{0.9\lambda}{B \cos \theta} \quad (2)$$

where,  $\lambda$  is the X-ray wavelength, B the angular line width at half maximum intensity and  $\theta$  the Bragg's angle. The dislocation density ( $\delta$ ) of the ZnO prepared was estimated using the equation (3)<sup>18</sup>.

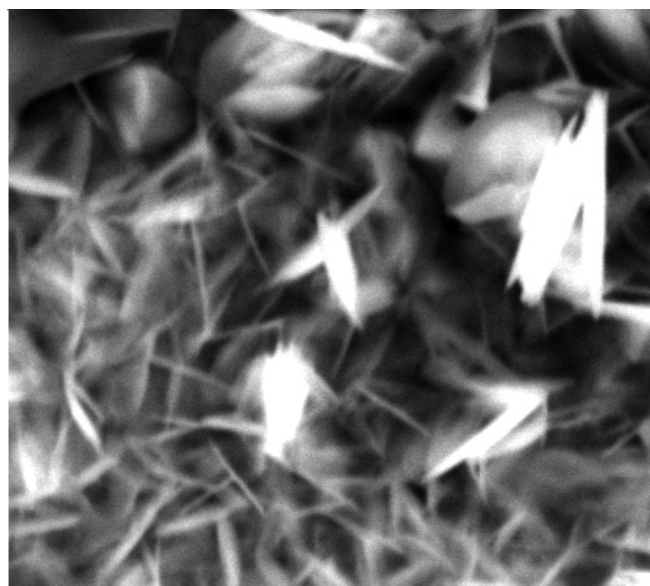
$$\delta = 1/D^2 \text{ (lines/m}^2\text{)} \quad (3)$$

The particle sizes calculated from scherrer formula and dislocation density values were shown in Table-2. Particle sizes were decreased with annealing, but dislocation density was increased with annealing.

TABLE-2  
CALCULATED "D" AND "δ" VALUES FOR ZnO

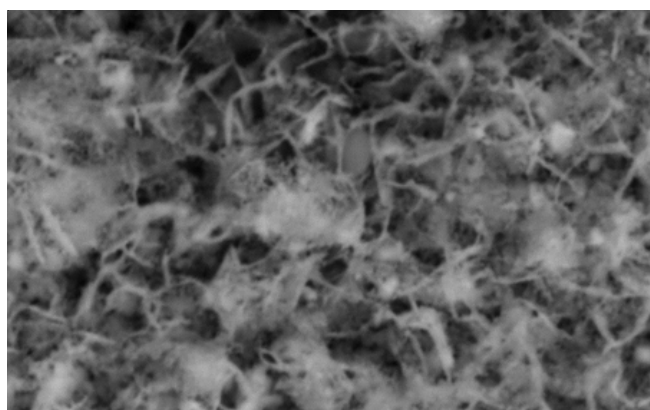
Sample	D (nm)	δ x10 <sup>14</sup> (lines/m <sup>2</sup> )
Unannealed ZnO	52.1	3.68
Annealed ZnO for 3h at 450 °C in air	28.9	11.9

The morphological properties of unannealed and annealed ZnO thin films were investigated by SEM analysis and SEM images were shown in Fig. 3. It was seen like nanowire structures at SEM images and we observed uniform morphology about 5 μm. Also, grains of ZnO were became small and colour of grains matt with annealing. This change in particle sizes of the values is in compliance with ones calculated by using Scherrer formula from XRD data.



5 μm

(a)



5 μm

(b)

Fig. 3. SEM images of the pattern (a) unannealed FTO/ZnO (b) annealed FTO/ZnO at 450 °C for 3 h

**Electrical properties:** To measure electrical properties, it was made of Au contact on annealed FTO/ZnO structure by sputter technique. For a schottky barrier diode (SBD), in the

presence of an interfacial layer and other effect the barrier height depends on the bias voltage; thermionic emission (TE) theory predicts that the current-voltage characteristic with the series resistance is thus given as follows<sup>19</sup>:

$$I = I_0 \left[ \exp\left(\frac{q(V - IR_s)}{nkT}\right) - 1 \right] \quad (4)$$

where,  $I_0$  is the saturation current derived from the straight line intercept of  $\ln I$  at  $V = 0$  and is given by:

$$I_0 = AA^* T^2 \exp\left(-\frac{q\phi_b}{kT}\right) \quad (5)$$

where,  $\phi_b$  is the effective barrier height at zero bias,  $A^*$  the Richardson constant, which equals 0.15 A/cm<sup>2</sup>K<sup>2</sup> for n-ZnO<sup>20</sup>.  $q$  is the electron charge,  $V$  is the forward-bias voltage,  $A$  the effective diode area,  $k$  boltzman's constant,  $T$  temperature in Kelvin and  $n$  is the ideality factor which is determined from the slope of the linear region of the forwards bias  $\ln I$ - $V$  characteristic by the relation:

$$n = \frac{q}{kT} \frac{dV}{d(\ln I)} \quad (6)$$

where,  $n$  is unity for an ideal diode. The ideality factor,  $n$ , is introduced to take into account the deviation of the experimental I-V data from the ideal TE model<sup>21</sup>. In this work,  $n$  is the ideality factor calculated from I-V characteristic using eqn. (6) and found to be 2.516 (Fig. 4a). This result greater than the ideal diode value. We can say that great  $n$  value can be caused forming oxide layer between the Au and ZnO layers.

The barrier height can be calculated from the equation:

$$q\phi_b = kT \ln\left(\frac{AA^* T^2}{I_0}\right) \quad (7)$$

The value of the  $\phi_b$  calculated from the I-V characteristic using eqn. (7). And  $\phi_b$  is found 0.953 eV (Fig. 4a). In order to calculated series resistance ( $R_s$ ) from I-V data eqn. (8) was used.

$$\frac{dV}{d(\ln I)} = IR_s + n \frac{kT}{q} \quad (8)$$

The results shown in Fig. 4b. The  $n$  and  $R_s$  values calculated and  $n$  was found 3.722 and  $R_s$  was found 3821Ω.  $R_s$  values greater than the other researches. The reason of high  $R_s$  may be the oxidation between Au and ZnO layers<sup>21</sup> and increase-ment in dislocation density depending on annealing effect. We can say the reason of the difference in ideality factor between Fig. 4a and b is using different methodes to find "n".

## Conclusion

Structural, morphological and electrical properties of electrodeposited ZnO were investigated. The XRD patterns showed fluorine doped tin(IV) oxide has a cassiterite and ZnO samples have a hexagonal structure. Lattice constant 'a' and 'c' calculated was harmonious with ones from PDF Card No: 36-1451. SEM images shown that all ZnO samples had like nanowire structure and a uniform morphology about 5 μm. According to calculated values from Scherrer Formula and SEM analysis, the particle sizes were decreased with annealing.

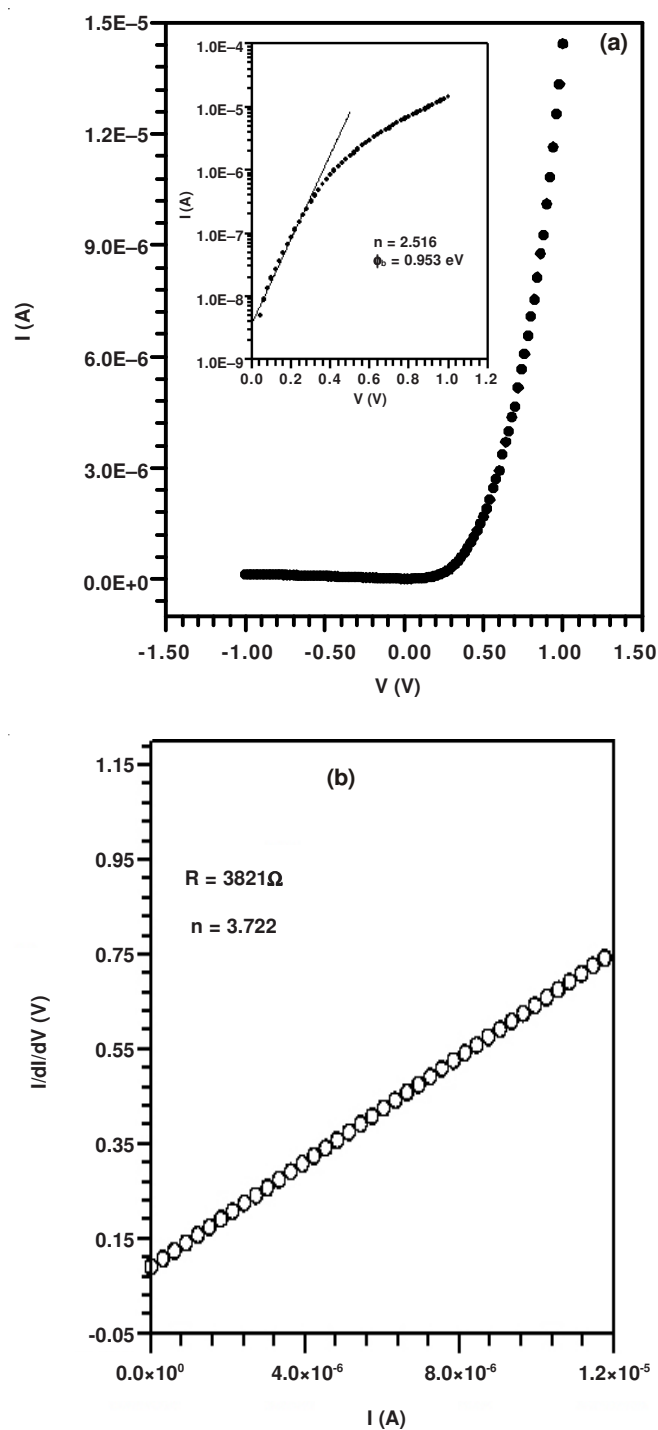


Fig. 4. a) Bias current-voltage characteristic for Au/ZnO contact b) A plot of  $dV/d(\ln I)$  data was obtained from forward bias current-voltage characteristics of the Au/ZnO contact

To investigation electrical properties, Au contact was made on FTO/ZnO structure. Au/n-ZnO schottky contact on fluorine doped tin(IV) oxide substrate characterized I-V technique. Obtained results shown that  $\phi_b$  barrier height 0.953 eV, n ideality factor 2.516 and serial resistance 3821  $\Omega$ . In this study, the reason emergence high ideality factor and serial resistance values may be thin oxide layer between the Au and ZnO. In summary, ZnO nanostructures on fluorine doped tin(IV) oxide successfully can be synthesized by electro-deposition and used as Schottky diodes.

#### ACKNOWLEDGEMENTS

The authors are grateful to the authorities of Ataturk University BAP for financial assistance the research project (No. BAP 2011/214).

#### REFERENCES

1. J.S. Wellings, N.B. Chaure, S.N. Heavens and I.M. Dharmadasa, *Thin Solid Films*, **516**, 3893 (2008).
2. G.-X. Miao, M. Munzenberg and J.S. Moodera, *Rep. Prog. Phys.*, **74**, 036501 (2011).
3. Z.L. Wang, *J. Phys.:Condens. Matter.*, **16**, R829 (2004).
4. A.E. Rakhshani, *Appl. Phys. A.*, **92**, 303 (2008).
5. T.M. Trad, K.B. Donley, D.C. Look, K.G. Eyink, D.H. Tomich and C.R. Taylor, *J. Cryst. Growth*, **312**, 3675 (2010).
6. N.-J. Kim, S. Choi, H.J. Lee and K.J. Kim, *Curr. Appl. Phys.*, **9**, 643 (2009).
7. I. Soumahoro, G. Schmerber, A. Douayar, S. Colis, M. Abd-Lefdil, N. Hassanain, A. Berrada, D. Muller, A. Slaoui, H. Rinnert and A. Dinia, *J. Appl. Phys.*, **109**, 033708 (2011).
8. D. Lincot, *Thin Solid Films*, **487**, 40 (2005).
9. K.B. Kumar and P. Raji, *Recent Res. Sci. Technol.*, **3**, 48 (2011).
10. E. Elangovan, S.A. Shivashankar and K. Ramamurthi, *J. Cryst. Growth*, **276**, 215 (2005).
11. K.S. Kim, S.Y. Yoon, W.J. Lee and K.H. Kim, *Surf. Coat. Technol.*, **138**, 229 (2001).
12. S. Chacko, N.S. Philip, K.G. Gopchandran, P. Koshy and V.K. Vaidyan, *Appl. Surf. Chem.*, **254**, 2179 (2008).
13. E. Elangovan, M.P. Singh and K. Ramamurthi, *Mater. Sci. Engg. B*, **113**, 143 (2004).
14. A.V. Moholkar, S.M. Pawar, K.Y. Rajpure, C.H. Bhosale and J.H. Kim, *Appl. Surf. Sci.*, **255**, 9358 (2009).
15. E. Elangovan and K. Ramamurthi, *Cryst. Res. Technol.*, **38**, 779 (2003).
16. J.S. Wellings, A.P. Samantilleke, P. Warren, S.N. Heavens and I.M. Dharmadasa, *Semicond. Sci. Technol.*, **23**, 125003 (2008).
17. V. Patil, A. Patil, J.W. Choi, Y.P. Lee, Y.S. Yoon, H.J. Kim and S.J. Yoon, *J. Electroceram.*, **23**, 214 (2009).
18. K. Ravichandran, G. Muruganatham and B. Sakthivel, *Physica B*, **404**, 4299 (2009).
19. E.H. Rhoderick and R.H. Williams, *Metal-Semiconductor Contacts*, Clarendon Press, Oxford (1988).
20. H. Sheng, S. Muthukumar, N.W. Emanetoglu and Y. Lu, *Appl. Phys. Lett.*, **80**, 2132 (2002).
21. S. Aydogan, K. Çinar, H. Asil, C. Coskun and A. Türüt, *J. Alloys Compounds*, **476**, 913 (2009).